NASA/TM—1998-208806

Thermomechanical Fatigue Durability of T650-35/PMR-15 Sheet Molding Compound

Michael G. Castelli
Ohio Aerospace Institute, Cleveland, Ohio

James K. Sutter
Lewis Research Center, Cleveland, Ohio

Dianne Benson
ProTech Lab Corporation, Cincinnati, Ohio

November 1998

The NASA STI Program Office . . . in Profile

Since its founding, NASA has been dedicated to the advancement of aeronautics and space science. The NASA Scientific and Technical Information (STI) Program Office plays a key part in helping NASA maintain this important role.

The NASA STI Program Office is operated by Langley Research Center, the Lead Center for NASA's scientific and technical information. The NASA STI Program Office provides access to the NASA STI Database, the largest collection of aeronautical and space science STI in the world. The Program Office is also NASA's institutional mechanism for disseminating the results of its research and development activities. These results are published by NASA in the NASA STI Report Series, which includes the following report types:

- TECHNICAL PUBLICATION. Reports of completed research or a major significant phase of research that present the results of NASA programs and include extensive data or theoretical analysis. Includes compilations of significant scientific and technical data and information deemed to be of continuing reference value. NASA's counterpart of peer-reviewed formal professional papers but has less stringent limitations on manuscript length and extent of graphic presentations.

- TECHNICAL MEMORANDUM. Scientific and technical findings that are preliminary or of specialized interest, e.g., quick release reports, working papers, and bibliographies that contain minimal annotation. Does not contain extensive analysis.

- CONTRACTOR REPORT. Scientific and technical findings by NASA-sponsored contractors and grantees.

- CONFERENCE PUBLICATION. Collected papers from scientific and technical conferences, symposia, seminars, or other meetings sponsored or cosponsored by NASA.

- SPECIAL PUBLICATION. Scientific, technical, or historical information from NASA programs, projects, and missions, often concerned with subjects having substantial public interest.

- TECHNICAL TRANSLATION. English-language translations of foreign scientific and technical material pertinent to NASA's mission.

Specialized services that complement the STI Program Office's diverse offerings include creating custom thesauri, building customized data bases, organizing and publishing research results . . . even providing videos.

For more information about the NASA STI Program Office, see the following:

- Access the NASA STI Program Home Page at ***http://www.sti.nasa.gov***

- E-mail your question via the Internet to help@sti.nasa.gov

- Fax your question to the NASA Access Help Desk at (301) 621-0134

- Telephone the NASA Access Help Desk at (301) 621-0390

- Write to:
  NASA Access Help Desk
  NASA Center for AeroSpace Information
  7121 Standard Drive
  Hanover, MD 21076

NASA/TM—1998-208806

Thermomechanical Fatigue Durability of T650-35/PMR-15 Sheet Molding Compound

Michael G. Castelli
Ohio Aerospace Institute, Cleveland, Ohio

James K. Sutter
Lewis Research Center, Cleveland, Ohio

Dianne Benson
ProTech Lab Corporation, Cincinnati, Ohio

Prepared for the
Symposium on Time-Dependent and Non-Linear Effects in Polymers and Composites
sponsored by the American Society for Testing and Materials
Atlanta, Georgia, May 4–5, 1998

National Aeronautics and
Space Administration

Lewis Research Center

November 1998

Acknowledgments

The authors would like to thank Mr. Chris Burke, Mr. Ralph Corner, Ms. Linda Inghram, Ms. Linda McCorkle, and Mr. Dan Scheiman for their expert technical assistance in the various laboratory facilities at NASA LeRC; Mr. Dennis Keller for assistance with the statistical planning aspects; Dr. Gary Roberts for helpful technical discussions and supplying the neat PMR-15 resin, and Mr. Kevin Kannmacher and Mr. Wayne Maple of AADC for fabricating and supplying the SMC panels.

Available from

NASA Center for Aerospace Information
7121 Standard Drive
Hanover, MD 21076
Price Code: A03

National Technical Information Service
5285 Port Royal Road
Springfield, VA 22100
Price Code: A03

Thermomechanical Fatigue Durability of T650-35/PMR-15 Sheet Molding Compound

Michael G. Castelli
Ohio Aerospace Institute
NASA Lewis Research Center
Cleveland, Ohio
USA

James K. Sutter
National Aeronautics and Space Administration
Lewis Research Center
Cleveland, Ohio
USA

Dianne Benson
ProTech Lab Corporation
Cincinnati, Ohio
USA

ABSTRACT: Although polyimide based composites have been used for many years in a wide variety of elevated temperature applications, very little work has been done to examine the durability and damage behavior under more prototypical thermomechanical fatigue (TMF) loadings. Synergistic effects resulting from simultaneous temperature and load cycling can potentially lead to enhanced, if not unique, damage modes and contribute to a number of nonlinear deformation responses. The goal of this research was to examine the effects of a TMF loading spectrum, representative of a gas turbine engine compressor application, on a polyimide sheet molding compound (SMC). High performance SMCs present alternatives to prepreg forms with great potential for low cost component production through less labor intensive, more easily automated manufacturing. To examine the issues involved with TMF, a detailed experimental investigation was conducted to characterize the durability of a T650-35/PMR-15 SMC subjected to TMF mission cycle loadings. Fatigue damage progression was tracked through macroscopic deformation and elastic stiffness. Additional properties, such as the glass transition temperature (T_g) and dynamic mechanical properties were examined. The fiber distribution orientation was also characterized through a detailed quantitative image analysis. Damage tolerance was quantified on the basis of residual static tensile properties after a prescribed number of TMF missions. Detailed microstructural examinations were conducted using optical and scanning electron microscopy to characterize the local damage. The imposed baseline TMF missions had only a modest impact on inducing fatigue damage with no statistically significant degradation occurring in the measured macroscopic properties. Microstructural damage was, however, observed subsequent to 100 h of TMF cycling which consisted primarily of fiber debonding and transverse cracking local to predominantly transverse fiber bundles. The TMF loadings did introduce creep related effects (strain accumulation) which led to rupture in some of the more aggressive stress scenarios examined. In some cases this creep behavior occurred at temperatures in excess of 150 °C below commonly cited values for T_g. Thermomechanical exploratory creep tests revealed that the SMC was subject to time dependent deformation at stress/temperature thresholds of 150 MPa/230 °C and 170 MPa/180 °C.

Introduction

High performance polymeric composites (PMCs) continue to be the focus of a number of research efforts aimed at developing cost effective, light weight material alternatives for advanced aerospace and aeropropulsion applications. These materials not only offer significant advantages in specific stiffness and strength over their current metal counterparts, but present the further advantage that structures can be designed and manufactured to eliminate joints and fasteners by combining individual components into integral subassemblies, thus making them extremely attractive for commercial applications. Of particular interest to elevated temperature applications, are polyimide matrix based composite materials which exhibit outstanding thermal stability providing for short and long term uses to 550 and 300 °C, respectively [*1*]. PMR-15 is one such polyimide which has seen considerable

use in aeropropulsion applications due to its good thermo-oxidative stability, relatively low cost and availability in a variety of forms [*2*].

With current emphasis on low cost manufacturing aspects of advanced composite structures, there is heightened interest on high performance sheet molding compounds (SMCs). SMCs effectively serve to reduce the costs associated with component production using prepregs, where variable costs are generally associated with labor, secondary processes and scrap. Using compression molding, SMCs can be molded into complicated shapes facilitating the use of simple charge patterns, part consolidation and molded-in inserts, which reduce labor, equipment, and operation costs for preparatory and secondary processes [*3*]. Specific to the present study is a carbon fiber reinforced PMR-15 SMC which has been used in a number of elevated temperature static aero applications, including oil exposed helicopter gearboxes [*2*] and shrouds for gas turbine engine-inlet housings [*4*].

The primary objective of the present research was to evaluate the durability of PMR-15 SMC subjected to a thermomechanical fatigue (TMF) loading spectrum. The TMF mission spectrum was representative of conditions found at a mid-stage within a gas turbine engine compressor. Researchers at Allison Advanced Development Company (AADC) and NASA Lewis Research Center investigated the use of PMR-15 SMC as the material comprising a mid-stage inner vane endwall [*5*]. Such a component resides in the engine flow path and is subjected to not only high airflow rates, but also elevated temperatures and pressures. Thus, the application represents a much more aggressive use of the material than those cited previously and raises obvious concerns related to the fatigue durability and damage tolerance. A survey of the literature on polyimide SMCs and their various applications reveals that very little information is available which details the structural durability of such materials, particularly in the light of more prototypical thermomechanical loading conditions. Therefore, one of the first goals of the current research was to determine reasonable maximum stress and temperature parameters for the representative engine mission cycle, so as to take full advantage of the SMC's capabilities.

Toward this end, a detailed experimental investigation was conducted to characterize the fatigue durability and damage tolerance of a T650-35/PMR-15 SMC subjected to TMF mission cycle loadings. Fatigue damage progression was tracked on the basis of longitudinal stiffness degradation and strain accumulation, while damage tolerance was quantified by residual static tensile properties after a prescribed number of TMF missions. The two parameters of stiffness and static response were selected not only because of application design and performance criteria, but due to their commonplace use in the area of damage mechanics and material life modeling [e.g., see ref. *6-9*]. Sufficient tests were conducted for all of the conditions investigated so that the statistical significance of the results could be assessed. Additional properties, such as fiber distribution orientation, glass transition temperature, T_g, and dynamic mechanical properties were examined. Detailed inspections were conducted using optical and scanning electron microscopy to characterize the microstructural damage. As the TMF cycle promoted damage associated with creep deformation, the creep behavior was investigated through a series of unique thermomechanical exploratory tests and compared with the response of neat PMR-15. Emphasis was placed on determining stress/temperature thresholds for time dependent deformation.

Material Details

Composition and Properties

The chopped carbon fiber polyimide based sheet molding compound examined in this study was T650-35/PMR-15 SMC [*10*] supplied by Quantum Composites, Inc., Midland, MI, (QCI 15C, lot # 092343; comparable to HyComp 310). The carbon fiber, Amoco's T650-35 (3K tow, UC309 sized), was chopped to 25 mm lengths and sprinkled with a randomized orientation (2-D) onto the matrix layer [see ref. *3* for details]. The composite panels had a nominal dimension of 10 x 20 x 0.22 (2 ply) cm and were compression molded at AADC, Indianapolis, IN, using the conditions presented in Table 1.

The T_g was measured on selected representative panels with an RMS 800 instrument (Rheometrics Scientific™) deforming the specimen in torsion at a frequency of 1 Hz, a temperature ramp rate of 5 °C/min, and a nominal specimen geometry of 40 x 5 mm (length x width). T_g was calculated by the intercept method using the storage modulus curve (for more details see ref. [*11*] pg. 245). The results indicated a dry T_g in the range of

284 to 306 °C which is generally considered to be unacceptably low for this material and indicative of insufficient postcuring. Therefore, all panels were subjected to a second postcure to raise the T_g. In an effort to optimize the T_g and also prevent extensive thermo-oxidative degradation, the effects of three potential secondary postcure cycles consisting of soaks at 316 °C in 1 atm air were evaluated. Specifically, test samples were postcured at 316 °C for either 4, 8, or 12 h. Prior to the secondary postcure, all panels were vacuum dried at 140 °C/76 cm Hg for 48 h. The average T_g values after the 4, 8, and 12 h postcures were 334, 339, and 345 °C, respectively. Given that the anticipated maximum test temperature would be approaching the target temperature of 316 °C, and desiring to test at a maximum temperature of at least 28 °C (i.e., 50 °F) below the T_g, the secondary postcure of 12 h at 316 °C was selected and implemented for all of the test panels.

The quality of all the postcured panels was evaluated by nondestructive analysis using ultrasonic C-scan. Past research in this area has successfully established a correlation between signal attenuation and void content [*12*]. Good consistency was found among the panels used in the study and C-scan results generally indicated void volumes in the range of 0.5 to 1.5 %. Additionally, the void content and fiber volumes were measured by the methods described in the *Test Method for Void Content of Reinforced Plastics (ASTM D 2734)* and *Test Method for Fiber Content of Resin-Matrix Composites by Matrix Digestion (ASTM D 3171)*. The void content and fiber volume values ranged from 0.9 to 1.7 % and 54 to 61 %, respectively. It is important to note that the fiber volumes are higher than those recommended for this type of SMC, which is generally desired to be in the range of 50 to 55 %. Fiber volume fractions above 55 % can lead to poor fiber wetting, reducing the overall mechanical performance of the material[1] (as will be seen in the discussion to follow).

Fiber Orientation Distribution

Carbon fiber orientation distribution has a significant effect on mechanical properties for SMCs. Therefore, a representative sample was subjected to a detailed examination to quantify the fiber orientation distribution at various depths into the thickness of the sample. This analysis was performed at ProTech Lab Corp., Cincinnati, OH. Fiber orientations at three depths (0.7, 1.0, and 1.5 mm) were examined through progressive polishing. The second depth represented the SMC's midsection. The area scanned was 218 mm^2 (approximately square) and was deemed to be representative of the plane. Fifty-five photographs, each representing approximately 3.95 mm^2, were used to compose the scanned area at each of the three depths. The detailed procedure for measuring the fiber orientation distribution is given in Appendix A.

The image analysis was performed by analyzing the carbon fiber distribution in 10 degree increments from 0 to 180 degrees, where the 0 and 180 degree orientations coincide and are parallel to the longitudinal specimen axis (i.e., the specimen loading axis). In theory, the fiber orientation in the plane being examined should be random for sheet molding compound composites. However, achieving a completely random distribution of carbon fibers during the prepreg process is very difficult. The image analysis results for depths 1 to 3 suggest that the carbon fiber distributions are not random, but rather, bi-modal. The fiber distributions through each of the three depths differ slightly, as might be statistically anticipated and depth 2 is only slightly bi-modal. However, depths 1 and 3 suggest a strong bi-modal distribution as illustrated Figure 1, where depth 3 is shown in histogram form. The bi-modal distribution tends toward fiber alignment along the longitudinal axis (i.e., 0 or 180 ±30 degrees), leaving a significantly reduced fiber volume fraction along the 90 ±30 degree axis. The tendency for such a trend is not entirely unanticipated by the manufacturers[1] given that the fibers are dropped onto the matrix sheet as it moves along on a conveyor system [*3*]. That is, the fibers tend to align in the moving direction, though a minimization of this tendency is desired and sought.

In addition to acid digestion, fiber volumes were determined by image analysis. The fiber volume percent at each depth was determined by randomly selecting ten digitized photographs at a magnification of 200x and assuming that the general bundle orientation had no effect on the fiber volume. The results from these fiber volume analyses are given in Table 2. Note that the values (56 to 61 %) correspond well to the fiber volumes obtained from acid digestion (54 to 61 %).

[1]Personal communication with Dr. Joseph Reardon, HyComp, Inc., Cleveland, OH, 44130.

Testing Details

All coupon specimens were cut using abrasive water-jet machining; each of the panels (10 x 20 cm) yielded three samples. After cutting and prior to testing, specimens were dried for 48 h at 140 °C and 76 cm Hg vacuum and then stored in a desiccator until immediately prior to testing. The specimen geometry was a reduced gage section dogbone geometry, shown in Figure 2. The relatively large radius of 36.8 cm forming the transition section has been used extensively in advanced metal matrix composite testing for a variety of laminates [*13*]. This geometry was successfully extended to high temperature PMC testing, facilitating gage section failures while avoiding the use of tabs [*14*].

The mechanical testing system was a closed-loop, servo-hydraulic system manufactured by MTS™ with a load capacity of 89 kN featuring hydraulic actuated, water cooled, diamond pattern serrated, wedge grips. Longitudinal strain measurements were obtained using an MTS™ air cooled extensometer with a 1.27 cm gage length mounted on the edge of the specimen. Specimens were heated using a quartz lamp system and actively cooled with forced air enabling the rapid thermal cycling necessary for the TMF cycle to be discussed. One of the formidable difficulties associated with true TMF testing (i.e., stress and temperature simultaneously dynamic) of PMCs is that of temperature measurement and control. Thus, a technique and control scheme were developed specifically for use with quartz lamp heating and PMCs [*14*]. First, a SMC temperature calibration specimen was manufactured with a series of internal K-type thermocouples (TCs) at known locations. This specimen was used to optimize the axial temperature gradients over the gage section to ±1 % of the nominal desired temperature. A K-type TC was then embedded in a block of neat PMR-15 and attached to the calibration specimen using a small metal mounting clip as shown in Figure 3a. Before each test, an externally mounted TC block was calibrated against the internal TCs of the SMC calibration specimen as illustrated in Figure 3b. The relationship between the imbedded and external TCs was found to be linear. The block was then mounted on a test specimen in the precise calibration location and used subsequently to measure and control the temperature. Repeatability of the relationship between the block and the calibration specimen was verified by removing and installing the setup several times and examining consistency; acceptable variations of ±2 °C were observed.

All static tensile tests were conducted in accordance with *the Standard Test Method for Tensile Properties of Plastics (ASTM D 638)* in displacement control with a loading rate of 0.5 mm/min. The TMF mission cycle used for this study is shown in Figure 4 (note that all loads are tensile). This generic cycle was determined by AADC researchers to be representative of the gas turbine compressor mid-stage inner vane endwall application. The mission consists of eight secondary segments, seven of which represent idle to maximum engine conditions, and one which represents a redline engine condition where the stress level is prescribed to be a 5 % increase over maximum. Note that the idle, maximum, and redline stresses and temperatures (σ^{I}, σ^{Max}, σ^{RL}, and T^{I}, T^{Max}, T^{RL}, respectively) are not specified, since determining these parameters was part of the research objective. Here, the goal was to determine a mission where the material was loaded as aggressively as possible, but survive a minimum of 100 h of mission cycling. As shown, the TMF mission time is approximately 50 minutes; therefore, 100 h of mission cycling corresponded to approximately 120 missions.

Once the TMF mission was specified, the test matrix consisted of testing to the two conditioning states of 50 and 100 h, in addition to the 0 hr TMF state which represents the unconditioned material. Residual tensile properties were then examined. A minimum of six tests was conducted at each of the TMF conditioning states satisfying issues regarding statistical significance. The experiments were intentionally designed with respect to *i*) order of tests and *ii*) specimen selection for condition. Given that each panel yielded three samples, one of each of these was used to examine the three conditioning states. For example, panel-A yielded samples A1, A2 and A3; A1 was used in a 0 h TMF residual test, A2 in a 50 h TMF residual test, and A3 in a 100 h TMF residual test. Thus, the design of experiments incorporated panel to panel variations for any one TMF state, but not specimen to specimen variation within a panel. The panel to panel variation was considered more significant. Several specimens were also tested to 50 and 100 TMF h states for purposes of destructive examination to detail the state of microstructural damage using optical and scanning electron microscopy.

Results and Discussion

Static Tensile Properties

One of the first issues to resolve on the PMR-15 SMC was the as-manufactured static properties. These properties would in-turn assist in formulating the maximum and redline parameters specified for the TMF mission cycle. Shown in Figure 5 are the room temperature (i.e., 22 °C) and 260 °C static tensile behaviors. The 22 and 260 °C tests yielded an average strength (σ^{ult}) of 259 and 230 MPa and an average strain to failure (ε^{f}) of 1.0 and 0.47 %, respectively. Two points were worthy of noting. First, the σ^{ult} values appeared to fall short of those advertised by the manufacturers of the comparable SMC, HyComp 310, (Dexter/HyComp) [*15*] by approximately 25 % at 22 °C and 17 % at 260 °C. This shortfall in tensile properties was likely due to the high fiber volume fraction state noted earlier. Further, the properties given in [*15*] were generated using four and six ply based materials, as opposed to two plies. The thicker materials will tend to show less scatter, as the through thickness characteristics become more homogeneous.

Second, note the distinctive "reverse" curvature (concave upward) of the tests performed at 260 °C indicative of a stiffening effect with increased loading. The curvature becomes markedly noticeable at an approximate stress/strain of 170 MPa/0.4 %. This effect is likely due to fiber straightening and/or rotation of the fiber segments into the loading direction, enabled by the viscous behavior of the matrix at 260 °C. This behavior was somewhat surprising, given that the temperature is significantly below the T_g (~ 337 °C). However, it will be discussed later in the exploratory creep deformation section that time dependent matrix deformation can be initiated at markedly low temperature values.

Given the apparently "viscous" response at 260 °C noted in Figure 5, a slightly lower temperature was examined for potential use as T^{Max} in the TMF cycle with the intent to avoid this type of deformation behavior as being typical for the mission cycle. However, the 260 °C target was felt to be a minimum for representing the T^{RL} condition. Shown in Figure 6 is the static tensile response at the slightly lower temperature of 232 °C. Having established, within the first few tests, that the stiffening effect was not manifested at this temperature, a full complement of tests was conducted (i.e., 6 repeats) to establish statistically meaningful static properties; these properties are also shown in Figure 6. Note there is a relatively large deviation in properties as one might expect with a SMC, particularly in view of the fiber orientation distribution information presented earlier. This variation was especially significant with regards to ε^{f}, where the standard deviation (Σ) was found to be approximately 25 % of the mean value. At a minimum, this suggests that the panel-to-panel variation in properties can be quite large.

Determination of TMF Capabilities and TMF Deformation

With T^{Max} specified to be 232 °C and T^{RL} established at 260 °C, the remaining key parameter to be determined was σ^{Max} (recall that σ^{RL} is specified at $1.05\sigma^{Max}$). As an initial estimate, the maximum fatigue stress was taken as (σ^{ult} - 3Σ) where σ^{ult} is taken at T^{Max}. Thus, the first set of TMF mission parameters featured σ^{Max} = 162 MPa with the remaining parameters, as shown in Table 3, where the stress values correspond to the column marked ($\sigma^{Max} = \sigma^{ult}$ - 3Σ). The specific idle parameters were selected as representative of the application without regard to the maximum and redline values. Also note that a σ^{Max} of 162 MPa represents a value corresponding to 72 % of σ^{ult}, a seemingly modest level in view of the fact that T^{Max} was more than 100 °C below T_g. A representative "cycle 1" deformation response for this TMF mission cycle is given in Figure 7, where the strain plotted is the total component (i.e., thermal and mechanical). As shown in Figure 7, the TMF cycle induces a relatively complex deformation behavior. Each of the secondary segments (idle to maximum) prior to the redline cycle is discernible as the material experienced a notable amount of creep deformation at maximum conditions. This effect is seen to decrease with progressive secondary segments as the material approaches a stabilized deformation response. When the redline condition was reached, the creep response was significantly revived, and then followed by a nominally elastic response corresponding to the remaining secondary segments of the mission cycle.

One obvious effect was the amount of strain recovery experienced within the cycle. For the test shown in Figure 7, a total creep strain of 0.14 % accumulated at maximum and redline conditions. However, after unloading from the final secondary segment, only 0.7 % (i.e., half) remained. Further, if time permitted, more strain would likely have been recovered. Unfortunately, the redline condition of σ^{Max} = 170 MPa at 260 °C proved to be too demanding to allow the full mission deformation response to stabilize. Note that the SMC mean ε^{f} (see Figure 6) at 232 °C is only slightly greater than that experienced after just one mission cycle. With progressive missions, a cyclic strain accumulation effect (comparable to creep ratchetting in metallic materials [*16*]) ensued leading to complete fracture of the sample. Although this test is revealing regarding material response under severe TMF conditions, the result prevented an important research objective: to establish residual properties subsequent to 100 h of TMF mission cycling. Therefore, TMF cycle revisions were necessary.

Shown in Figure 8 is the final modified TMF mission cycle which was used for all residual properties. This cycle was based upon stress parameters defined by $\sigma^{Max} = \sigma^{ult} - 4\Sigma$. The values for σ^{Max} and σ^{RL} were reduced to 143 and 150 MPa, respectively, with all other parameters held constant (see Table 3). This σ^{Max} value represents 64 % of σ^{ult} at 232 °C. Representative deformation responses of the SMC to this mission cycle are given in Figure 9, where both cycles 1 and 120 are shown. Several dramatic changes in the deformation behavior are noted when compared to that observed in Figure 7. First, the stress/strain response is seen to be essentially linear elastic, with only modest time dependent effects observable within a given cycle. Further, the viscous effects appear to be well stabilized within a given mission cycle with the redline condition having a seemingly inconsequential effect on the overall deformation behavior. Note that the material continues to experience a minor degree of permanent strain ratchetting on the order of 0.05 to 0.1 % strain, which tends to accumulate during the early cycles. Having determined that the T650-35/PMR-15 SMC was capable of sustaining the new mission cycle loading for 100 h, the full complement of tests was conducted to the 50 and 100 h states of conditioning and then checked for residual properties.

Residual properties

As indicated earlier, progressive fatigue damage accumulation was tracked through monitoring elastic stiffness degradation and damage tolerance was quantified on the basis of the static tensile property retention. Shown in Figure 10 are the elastic stiffness values measured as a function of accumulated TMF missions. These values were measured isothermally at 232 °C (i.e., T^{Max}) by applying a small elastic load (35 MPa) immediately after each mission cycle. Given the relatively large deviation in elastic stiffness (see Figure 6), to facilitate specimen-to-specimen comparison, this property was normalized with respect to the original value measured prior to testing. The one major conclusion drawn from this data is that the TMF mission cycling had little to no effect on elastic stiffness. Of the 12 tests shown, six were cycled to 60 and 6 were cycled to 120 mission cycles, the data divide essentially equally above and below the original value, indicating the lack of a clear or overriding trend. Further, the data from Figure 10 indicates that the modest changes observed are incurred early in the cyclic conditioning (prior to ~ 20 TMF missions) with only minimal exceptions. Subsequent to these early changes, the material tends to be cyclically neutral with respect to stiffness changes. The early changes may be indicative of a slight degree of fiber straightening, corresponding to the observed strain ratchetting and/or substructural damage (discussed later). Also note, in Figure 10, identical symbols represent specimens taken from the same original panel: one tested to 60 missions and the other tested to 120 missions. No panel-specific patterns corresponding to elastic stiffness degradation were observed.

Shown in Figure 11 are residual static tensile properties at 232 °C after 50 and 100 h of mission cycling (six tests for each condition); the 0 hour results from Figure 6 are also shown for comparison. Though the figure is relatively crowded and difficult to distinguish single tests, it serves to show the significant spread and/or grouping associated with the data. Also given in Figure 11 are the means ($\overline{\mathbf{X}}$) and standard deviations (Σ), for ultimate strength, strain to failure, and elastic stiffness. By comparing the $\overline{\mathbf{X}}$ and Σ values for the two populations (i.e., post 50 and 100 hour TMF conditions) through an analysis of variance to the 0 TMF h material behavior, it was determined that there were no significant differences at the 95 % confidence level in any of the three properties. The only property which exhibits a potential difference is the Σ of elastic stiffness for the 100 hour TMF condition,

which was significant at 92.5 % confidence level, but not at the 95 % level. This increased Σ over that exhibited prior to TMF cycling is consistent with the trend revealed in Figure 10, where some of the material tends to stiffen slightly and some tends to become more compliant, but the overall mean remains constant. Similar to the progressive stiffness changes discussed above, panel-specific trends associated with residual static tensile properties were examined and none were evident.

Another residual property examined was T_g — to check for potential aging. It is well known that elevated temperature exposures can advance the cure states of polyimides, potentially introducing changes in mechanical properties. The result indicated no change in T_g after 100 h of TMF mission cycling, which was anticipated given that the total time spent at 232 and 260 °C was 35 and 5 h, respectively. This observations is consistent with studies conducted on PMR-15 composites where volume changes were not found to occur after 100 h at 316 °C [*17*] and T_g was found to be stable up to 2000 h of exposure at 260 °C [*18*]. Thus, given the modest exposure times in the present study, it was assumed that the material did not incur any noteworthy aging.

Microstructural Examination

Microstructural examinations were conducted on several specimens subjected to TMF mission cycling. Although there was only minimal indication of damage corresponding to the macroscopic property degradation, there was clear evidence of highly localized damage at the microstructural level which was not evident in the untested control samples. Damage was predominantly associated with fiber/matrix interface de-bonding at fibers oriented at angles of 90 ±40 degrees, where the specimen longitudinal axis coincides with 0 or 180 degrees, that is, the loading direction. At points where such de-bonded fibers intersected with other fibers or fiber bundles having a different orientation, the cracks appear to have propagated from one bundle to the next, but generally remained confined to fibers oriented in the range specified above. This common pattern is well illustrated in Figure 12a where a surface-visible crack is seen in the presence of at least two fiber orientations (upper portion of picture). The crack likely initiated at the fiber interface oriented at approximately 105 degrees, then connected with the fibers oriented at approximately 60 degrees and proceeded to cause a localized interface de-bond along this orientation, albeit, in much less aggressive fashion. As would be expected, whenever a crack at a fiber intersection such as this is noted, the more dominant crack is generally associated with the fiber orientation closest to 90 degrees. Note that there is a third dominant fiber bundle orientation visible in the lower portion of the photograph where a starting crack is also associated; the orientation is approximately 135 degrees.

In general, it appears that when the crack front encountered a bundle with a predominant longitudinal (PL) orientation, the fiber bundle effectively bridged the crack, leading to cases where the crack propagated "around" the bundle to another having a predominantly transverse (PT) orientation. This "around" crack path was seen to be associated either with the cut end or the outer diameter of the PL bundle. An example of the first is shown in Figure 12b looking into the specimen thickness, where PT oriented fibers appear with a near circular cross-section, and PL oriented fibers appear elliptical. The crack shown here, connected to the surface, appears to propagate transverse to the loading direction through the PT bundles, but takes a path around the cut end of the PL bundle. Thus, in general, a through-thickness view of the SMC such as that shown in Figure 12c revealed the vast majority of transverse cracks in PT bundles. Further, there is an indication of damage progression from the 50 to the 100 hour TMF state, associated with higher transverse crack densities in the PT bundles, though the number of samples viewed (two for each case) was not sufficient to make a quantitative assessment. These microstructures do suggest, however, that given sufficient TMF cycling (significantly more than 100 h), the damage processes would eventually cause degradations in the macroscopic properties.

Fracture surfaces of residual strength specimens for all conditions (0, 50, and 100 h of TMF) appeared similar and are well represented by the fractography in Figure 13. The fracture surface was generally transverse to the loading direction and revealed features dominated by pull-out of PL fibers/fiber bundles and separating of PT fiber bundles. The pull-out did not appear to be influenced by ply to ply interfaces, which were generally indistinguishable, both on the fracture surfaces and on the polished mounts. Thus, there was no indication of ply-to-ply delamination. A number of bundles having PL orientations reveal some degree of fiber fractures, but this

effect appeared secondary to the pull-out feature. The general features were consistent with those cited by Beaumont and Schultz [*19*] for a room temperature fatigue failure of SMC-65.

Creep Response

During the process of determining the SMC's structural capabilities under TMF mission cycle loading, it became obvious that the more aggressive parameters investigated, which led to "premature" specimen fracture, induced a primary failure mode associated with creep deformation. This was facilitated by the fact that the TMF mission cycle featured a series of elevated temperature stress holds (2.5 min each), allowing for creep. This "excessive" creep was unanticipated given that the mission maximum and redline temperatures (232 and 260 °C, respectively) were significantly below the average T_g of approximately 340 °C, raising concerns associated with the time dependent deformation response.

Recently, some emphasis has been placed on characterizing the creep response of carbon fiber/polyimide PMCs because of long-term durability issues [e.g., refs. *17,20,21*], however, the work has been dominated by examining the effects of thermal aging at temperatures much closer to the material's T_g. Further, such investigations have dealt with continuous fiber reinforced materials, the much more common application. For PMR-15 SMC, the following questions needed to be addressed: At what stress/temperature threshold levels does creep occur? Further, do behaviors determined from routine dynamic mechanical loadings (e.g., storage and loss modulus, T_g, … etc.) give insight into thresholds for time dependent responses? A concise exploratory examination was conducted to address these critical issues.

Thermomechanical Creep Initiation — A novel thermomechanical creep deformation test was conducted where the temperature was ramped at 5 °C/min to the redline temperature with an applied static load. The temperature ramp rate was felt to be sufficiently slow so as to allow for a quasi static thermal equilibrium through the thickness of the sample. A preliminary test was conducted under zero load to assess the free thermal expansion of the SMC during the temperature ramp. The specimen was then loaded at the redline stress level and subjected to the same temperature excursion. The goal of this test was to identify the temperature at which creep initiated. The results of this test are shown in Figure 14 for two different conditions consisting of the two redline levels discussed previously. The creep strain plotted was reduced by subtracting off the time independent elastic and thermal strain components. As seen in Figure 14, with the nominal σ^{RL} of 150 MPa applied, the creep threshold was determined to be approximately 230 °C. Further, the experiment revealed that the creep response at the redline temperature of 260 °C, remains relatively modest. Note that 230 °C essentially corresponds to the TMF mission cycle T^{Max}, at which point the stress is slightly less. These results correspond well to the deformation behaviors observed during the (-4Σ) TMF mission cycling, indicating that the creep experienced at maximum and redline conditions should be minimal. The creep threshold temperature drops quickly, however, when the creep stress level is set to the more demanding σ^{RL} of 170 MPa. Under these conditions creep deformation is found to initiate at approximately 180 °C which is well below both the T^{Max} and T^{RL}. Again, the results here are consistent with the excessive creep observed during the exploratory phase of establishing TMF capabilities; recall Figure 7. The data suggest that if a σ^{RL} of 170 MPa is to be tolerated, then the T^{RL} need be restricted to approximately 230 °C. It is important to note that the creep deformations experienced were strictly associated with a viscoelastic response (no microstructural damage) and verified to be fully reversible/recoverable.

To gain further insight into the creep threshold temperature of the SMC, a comparable test was conducted on the neat PMR-15 resin with an identical post-cure cycle. The results are given in Figure 15. The thermomechanical threshold stress for temperatures below 260 °C was found to be ~21 MPa, which is seen to initiate creep at 240 °C. By examining the tensile strength of the neat PMR-15 it was determined that this stress level corresponds to ~56 % of the material σ^{ult} at 260 °C. A stress/temperature viscoelastic threshold "lower-bound" was estimated for neat PMR-15 by Kamvouris, et al. [*11*] to be approximately 204 °C, with stress levels up to 50 % of σ^{ult}. This was concluded because no creep strains were observed over time periods approaching 720 h. The data presented in Figure 15 agrees and further defines this stress/temperature creep threshold, suggesting that for a temperature of 204 °C as proposed by Kamvouris et al., a stress level approaching 70 % of σ^{ult} would be needed to induce time

dependent deformation. Having established this threshold, a stress level corresponding to 64 % of the 260 °C σ^{ult} (i.e., 24 MPa) was applied to examine a macroscopic stress level "comparable" to that being applied to the SMC (i.e., 150 MPa). The results indicated that the neat PMR-15 resin experienced creep initiation at approximately 215 °C. It should be noted that the "comparable" stress comparison between the neat resin and SMC materials is not to suggest an identical stress state. Unlike the neat resin, the localized matrix in the SMC is subjected to a highly complex multiaxial stress state. Further, use of the respective σ^{ult} values as the normalizing factors reflects only modest mechanistic relevancy, as these parameters are dictated by significantly different failure mechanisms for the two classes of materials. However, it remains noteworthy that the PMR-15 resin behavior clearly indicates that at mid-stress levels (50 to 70 % σ^{ult}), time dependent deformation is likely to occur at temperatures as low as 200 °C: *a temperature which is nominally 150 °C below commonly cited T_g values.* The creep response measured on the neat matrix confirms the low temperature creep deformation exhibited by the SMC, where the characteristic creep behavior is dictated by the properties of the PMR-15. Also, if the possibility of interface damage associated with PT fibers is considered, both the creep threshold and creep rates may be detrimentally affected, giving rise to properties that are even less desirable than those of the matrix alone. Such an effect of "structural weakening" is relatively common in cases of transversely reinforced systems, and has been noted with specific reference to elevated temperature creep behavior of polyimide based composites [*22*].

Dynamic Mechanical Response — A final aim of the exploratory SMC creep investigation was to relate the thermomechanical creep thresholds to dynamic mechanical characterizations routinely performed on polymers and their composites to determine T_g. Specifically, does the dynamic mechanical response provide *quantitative* insight to the thermomechanical creep threshold? It is well known in the polymer science field that temperature dependent dynamically measured properties (e.g., storage modulus, loss modulus ,T_g, … etc.) are not time independent properties, but rather vary as functions of both temperature rate and loading rate. This fact, however, is often overlooked or at least minimized by mechanics researchers, who generally tend to treat and report material properties, such as T_g, as unique, time independent values (like melting points). Such issues of time dependency are central to the consideration of a thermomechanical creep threshold.

A series of dynamic mechanical characterization curves for the SMC and neat PMR-15 are shown in Figures 16 and 17, respectively. The loading rate dependency was examined over the range from 0.1 to 10 rad/sec using the RMS 800 (Rheometrics™). The temperature sweep rate was maintained constant at 5 °C/min for all of the tests and the T_g values were determined by the intercept method from the storage modulus as before. All of the samples used for this examination were taken from the same panel with the goal of minimizing material variability, while highlighting the effects of time dependency. The T_gs of both the SMC and neat PMR-15 were found to vary considerably with loading frequency. The shear loss modulus, G″, representative of the imaginary part of the complex modulus, is usually discussed in the context of its maximum at the α transition, by which the T_g is often defined. However, this "out-of-phase" component is also indicative of sub-T_g transitions, or more subtle viscous effects pertinent to the discussion of time dependency.

As the temperature progresses from ambient conditions, G″ experiences a local minimum and then increases as the α transition is approached. The significant observation in Figures 16 and 17 is that the approximate temperature at which the increase in G″ occurs, decreases with decreasing loading rate, showing a typical positive strain rate dependence. For clarification, each of the local increase points are designated with an "I" on the plots. Though this observation is not uncommon, such behavior is generally not discussed in the context of defining the onset of time dependent behavior. Note that as the loading rate is decreased, the state begins to approximate a static load condition, facilitating a comparison with the static load thermomechanical creep threshold tests. The G″ trends indicate that it is not unreasonable to expect time dependent deformation at temperatures as low as approximately 200 °C, which is in the range of 150 °C below commonly cited T_g values for PMR-15 and its composites. This result compares well with the findings from the exploratory thermomechanical creep threshold experiments. The fact that time dependent behavior can be experienced at such modest temperatures needs to be highlighted when considering the long term use of these materials in deformation critical applications.

Summary/Conclusions

A detailed experimental investigation was conducted to characterize the thermomechanical fatigue (TMF) durability and damage behavior of the carbon fiber/polyimide sheet molding compound (SMC), T650-35/PMR-15. High performance SMCs present alternatives to prepreg forms with great potential for low cost component production. The TMF loading spectrum was proposed by Allison Advanced Development Company to be representative of a gas turbine engine compressor application where the SMC will be used for an inner vane endwall. The fiber distribution orientation was characterized through detailed quantitative image analyses, revealing a non-randomized fiber distribution orientation. Mechanical damage progression was tracked macroscopically on the basis of property changes, in addition to examining other properties such as glass transition temperature, T_g, and dynamic mechanical properties. Damage tolerance was quantified through residual static tensile properties after a prescribed number of TMF missions. Detailed microstructural examinations were conducted using optical and scanning electron microscopy to characterize the local damage. The SMC was further evaluated through a series of exploratory thermomechanical creep tests designed to determine stress/temperature creep thresholds. Similar thermomechanical tests on the neat PMR-15 resin permitted a comparison of the creep characteristics to the PMR-15 SMC.

The imposed TMF missions were found to have only a modest impact on inducing fatigue-type damage when limiting the exposure to 100 h. Microstructural damage was observed after 50 and 100 h of TMF cycling which consisted primarily of fiber debonding and transverse cracking local to various fiber bundles. However, no statistically significant degradations occurred in the elastic stiffness, or the residual properties of strain to failure and ultimate tensile strength. The TMF loadings did, however, promote creep damage and excessive strain accumulation which led to rupture in more aggressive stress scenarios. The creep behavior was found to occur in some cases at temperatures more than 150 °C below glass transition temperatures commonly cited for PMR-15 composites. Thermomechanical exploratory creep tests revealed that below 260 °C (the redline temperature investigated) the SMC undergoes time-dependent deformation at the stress/temperature threshold level of 150 MPa/240 °C. Stress increases above this level allowed for lower temperature thresholds in the range of 180°C. Finally, upon examining relatively slow loading rates during dynamic mechanical testing, trends revealed by the loss modulus (G″) were found to serve as good indicators of the creep threshold temperatures.

APPENDIX A

Procedure for Quantitative Image Analysis of the Fiber Orientation Distribution

1. Metallographic images were captured in gray scale from a video monitor/computer which is connected to a camera in the Nikon metallograph. A magnification of 50x was used to capture images across the entire cross section. The images were then imported to NIH Image Analysis program where the images were "seen as" 320 x 240 pixels (video squares) each with a level of gray between 0 and 255 (0=white, 255=black).

2. The images were calibrated against a known standard so that measurements could be made in millimeters.

3. The angle tool within the image analysis program was used to measure the predominant orientation of fibers within a fiber bundle region. The freehand tool was then used to outline this region to measure its geometric area. A MS Excel spreadsheet was used to record all measurements.

4. All fiber bundle regions at each cross section were analyzed. The total area of the fiber bundle regions within each orientation category was calculated. The fiber volume percent within the fiber bundles was taken into account to calculate the overall fiber volume orientation distribution.

References

[1] Wilson, D., "Polyimides as Resin Matrices for Advanced Composites," *Polyimides*, Wilson, D. Stenzenberger, H.D. and Hergenrother, P.M., Eds. Chapman and Hall, 1990, pp. 187-226.

[2] Stevens, T. "PMR-15 is A-OK," *Materials Engineering*, Oct. 1990, pp. 34-38.

[3] Allen, P. and Childs, B., "SMC: A Cost Effective Alternative to Prepreg Technology, *38th International SAMPE Symposium*, 1993, pp. 533-46.

[4] Hoff, S.M., "Applying Advanced Materials to Turboshaft Engines," *Aerospace Engineering*, Vol. 15, No. 2, 1995, pp. 27-30.

[5] *Investigation of Low Cost High Temperature PMC Components*, NASA Contract NAS3-97015, 1997.

[6] Hahn, H.T. and Kim, R.Y., "Fatigue Behavior of Composite Laminate," *Journal of Composite Materials*, Vol. 10, 1976, pp. 156-80.

[7] Talreja, R., "Stiffness Based Fatigue Damage Characterization of Fibrous Composites" *Fatigue of Composite Materials*," Technomic Publishing Company, Lancaster, Pennsylvania, 1987, pp. 73-81.

[8] Yang, J.N. and Liu, M.D., "Residual Strength Degradation Model and Theory of Periodic Proof Tests for Graphic/Epoxy Laminates," *Journal of Composite Materials*, Vol. 11, 1977, pp. 176-203.

[9] Reifsnider, K.L. and Stinchcomb, W.W., "A Critical Element Model of the Residual Strength and Life of Fatigue-Loaded Composite Coupons," *Composite Materials: Fatigue and Fracture, ASTM STP 907*, H.T. Hahn, Ed., ASTM, Philadelphia, 1986, pp. 298-303.

[10] Reardon, J.P. and Thorpe, J.D., U.S. Patent No. 5126085 920630, 30 Jun. 1992.

[11] Kamvouris, J.E., Roberts, G.D., Pereira, J.M. and Rabzak, C., "Physical and Chemical Aging Effects in PMR-15 Neat Resin," *High Temperature and Environmental Effects on Polymeric Composites: 2nd Volume, ASTM STP 1302*, Thomas S. Gates and Abdul-Hamid Zureick, Eds. ASTM 1997, pp. 243-58.

[12] Roth, D.J., Baaklini, G.Y., Sutter, J.K., Bodis, J.R.,, Leonhardt, T. and Crane, E.A., "NDE Methods Necessary for Accurate Characterization of Polymer Matrix Composite Uniformity, *Advanced High Temperature Engine Materials Technology Program*, NASA CP 10146, 1994, paper 11.

[13] Castelli, M.G., "A Summary of Damage Mechanisms and Mechanical Property Degradation in Titanium Matrix Composites Subjected to TMF Loadings," *Thermal-Mechanical Fatigue of Aircraft Engine Materials*, AGARD Conference Proceedings 569, Mar., 1996, pp. 12:1-12.

[14] Gyekenyesi, A.L., Castelli, M.G., Ellis, J.R., and Burke, C.B., "A Study of Elevated Temperature Testing Techniques for the Fatigue Behavior of PMCs: Application to T650-35/AMB-21," NASA TM-106927, July 1995.

[15] Dexter Composites Division Data Sheet for HyComp M-300 Series Sheet Molding Compound, Dexter Corporation (now HyComp, Inc.), Cleveland, Ohio.

[16] Skrzypek, J.J., *Plasticity and Creep: Theory, Examples, and Problems*, R.B. Hetnarski, Ed, CRC Press, Inc., Boca Raton, FL, 1993, p. 128.

[17] Skontorp, A. and Wang., S.S., "High-Temperature Aging, and Associated Microstructural and Property Changes in Carbon -Fiber Reinforced Polyimide Composites, *Proceedings of the 9th technical Conference of the American Society of Composites*, Technomic Pub., 1994, pp. 1203-12.

[18] Bowles, K.J., Roberts, G.D. and Kamvouris, J.E., "Long-Term Isothermal Aging Effects on Carbon Fabric-Reinforced PMR-15 Composites: Compression Strength," *High Temperature and Environmental Effects on Polymeric Composites: 2nd Volume, ASTM STP 1302*, Thomas S. Gates and Abdul-Hamid Zureick, Eds. ASTM 1997, pp. 175-90.

[19] Beaumont, P.W.R. and Schultz, J.M., "Fractography," *Failure Analysis of Composite Materials: Delaware Composites Design Encyclopedia*, Vol. 4, 1990, pp. 134-35.

[20] Pasricha, A., Dillard, D.A. and Tuttle, M.E., "Effect of Physical Aging and Variable Stress History on the Creep Response of Polymeric Composites," *Mechanics of Plastics and Plastic Composites*, ASME, MD-Vol. 68/AMD-Vol. 215, 1995, pp. 283-99.

[21] Brinson, L.C. and Gates, T.S., "Effects of Physical Aging on Long-Term Creep of Polymers and Polymer Matrix Composites, *International Journal of Solids and Structures*, Vol. 32, No. 6, 1995, pp. 827-46.

[22] Rodeffer, C.D., Maybach, A.P. and Ogale, A.A., "Influence of Thermal Aging on the Transverse Tensile Creep Response of a Carbon Fiber/Thermoplastic Polyimide Composite," *Journal of Advanced Materials*, Jan. 1996, pp. 46-51.

TABLE 1—T650-35/PMR-15 SMC panel processing details.

Imidization Cycle	Cure Cycle	Postcure Cycle
• Room temperature to 121 °C over 30 min • Hold at 121 °C for 30 min • Ramp to 204 °C over 30 min • Hold at 204 °C for 1 hr	• Preheat mold to 260 °C • Load imidized part into mold • Close mold, apply no pressure and wait 2 minutes • Apply 4.1 MPa and heat mold to 316 °C • Hold pressure and heat for 60 min • Cool while maintaining 4.1 MPa until mold temp is 204 °C and unload part	• Heat from room temperature to 249 °C over 3 hr • Hold at 249 °C for 3 hr • Ramp to 288 °C over 2 hr • Hold at 288 °C for 3 hr • Ramp to 316 °C over 2 hr • Hold at 316 °C for 12 hr • Cool to room temperature over 6 hr

TABLE 2—Fiber volume percentages determined by quantitative image analysis.

Polishing Depth	Fiber Volume, %
1	60.6
2	56.4
3	55.7

TABLE 3 —Temperature and stress values for TMF mission cycle.

Engine Condition	Temperature, °C	Stress, MPa ($\sigma^{MAX} = \sigma^{ult} - 3\Sigma$)	Stress, MPa ($\sigma^{MAX} = \sigma^{ult} - 4\Sigma$)
Shutdown	26	0	0
Idle	123	36	36
Maximum	232	162	143
Redline	260	170	150

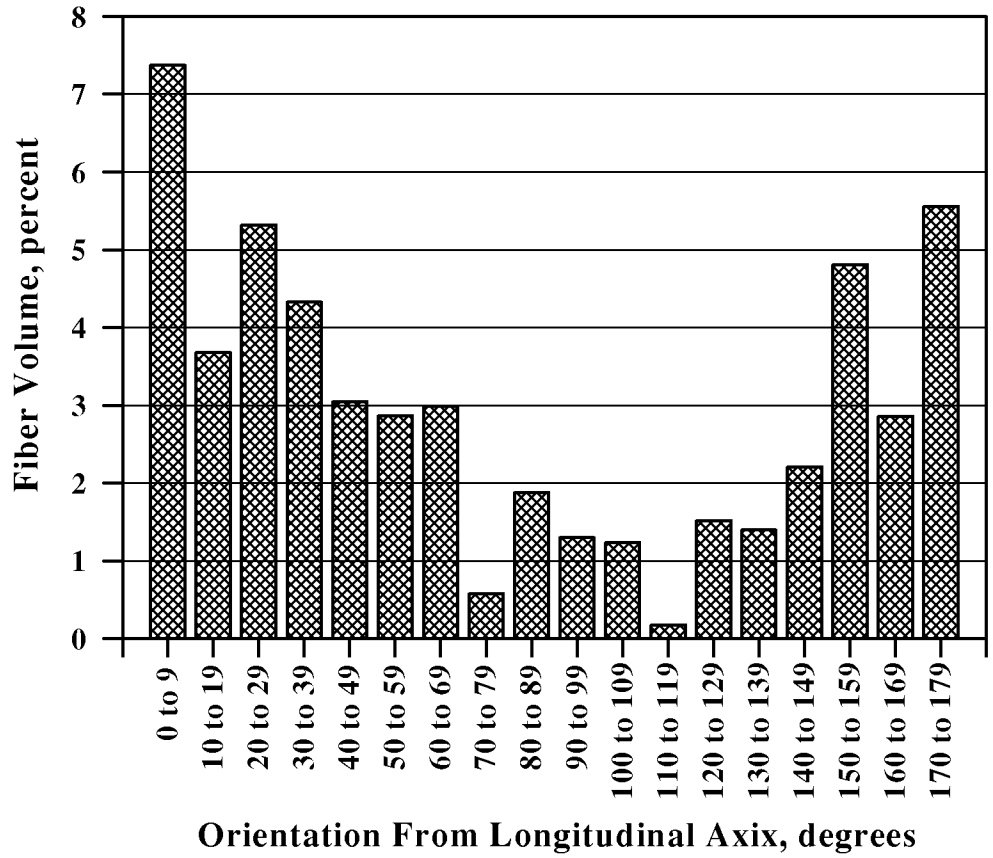

Figure 1—Fiber orientation distribution found at depth 3 (1.5 mm into thickness) revealing strong bi-modal trend.

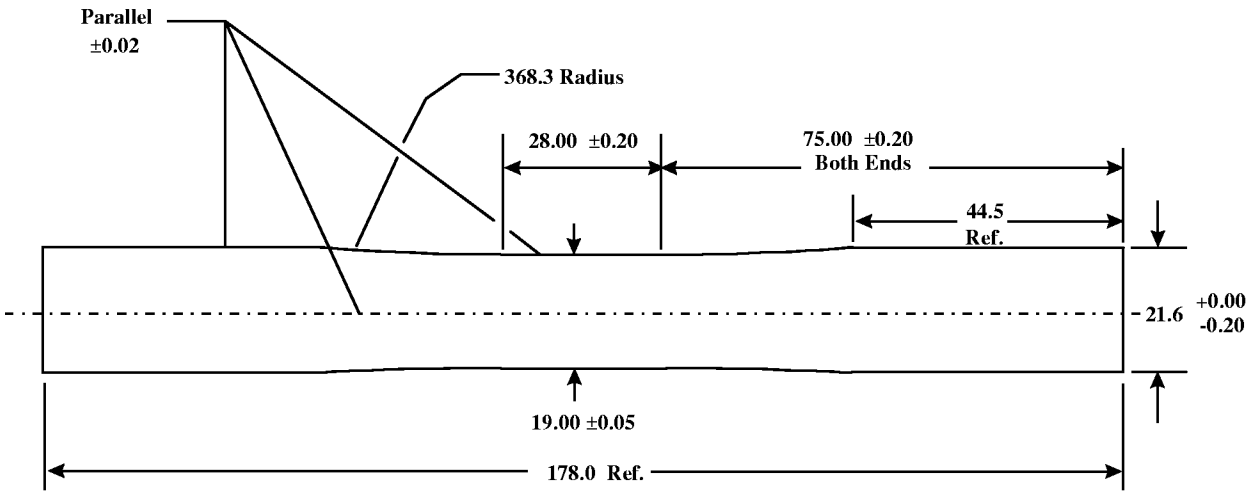

Figure 2—Specimen geometry for tensile and TMF tests.

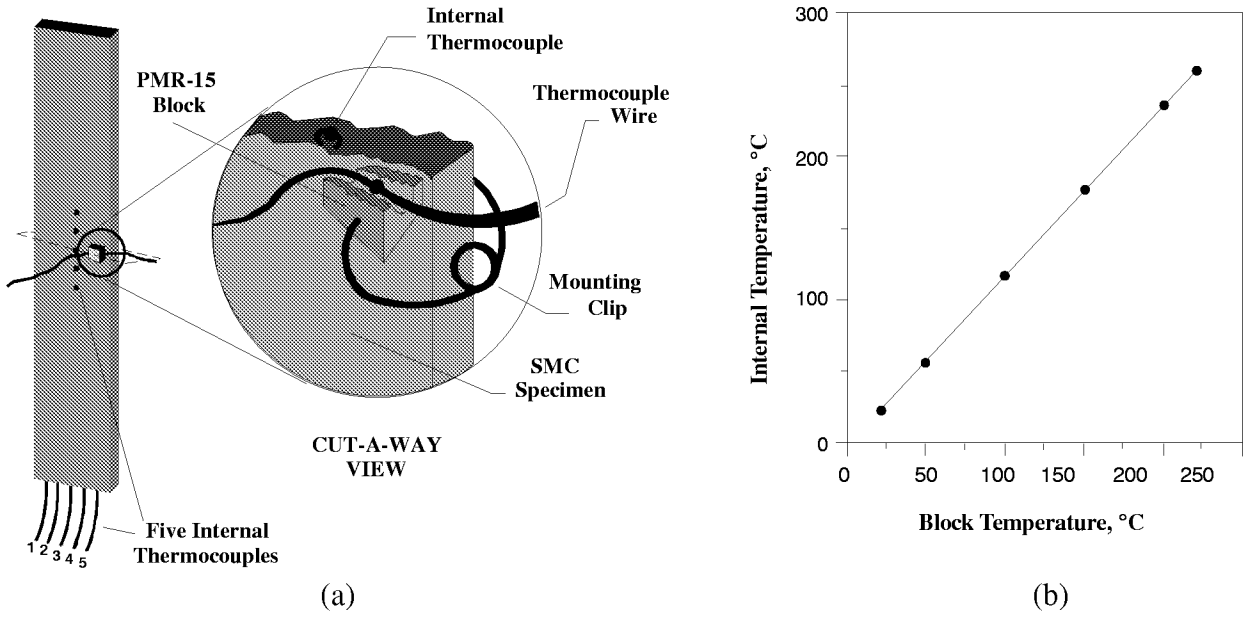

Figure 3—Temperature measurement and control scheme showing (a) the internal and external block thermocouple configuration and (b) representative calibration data.

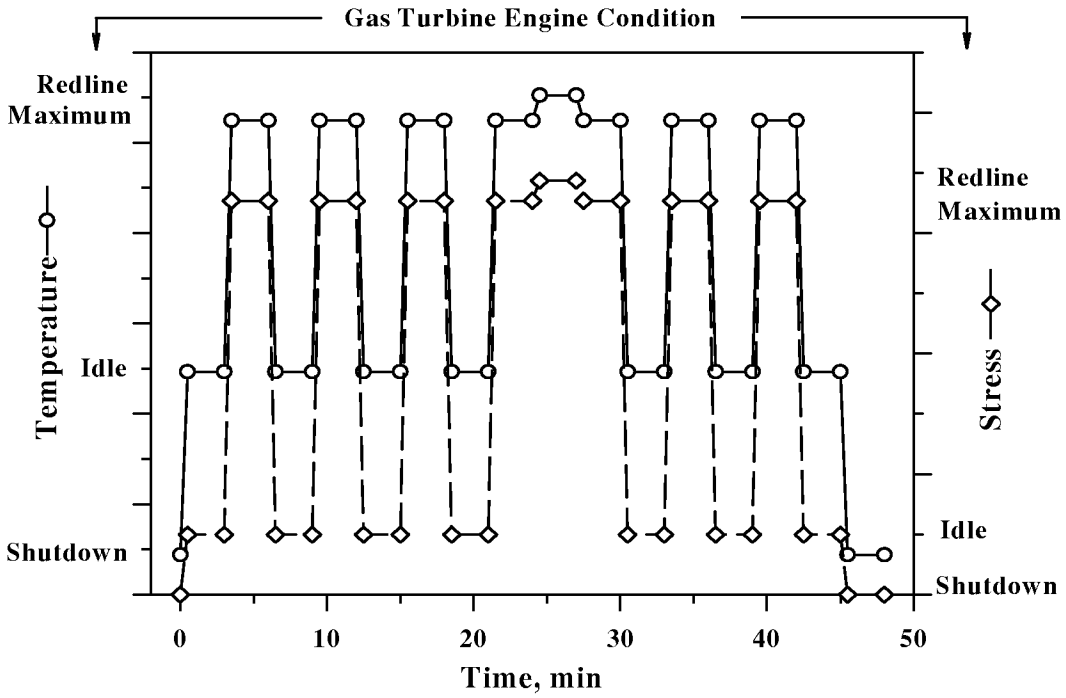

Figure 4—TMF mission cycle representative of a gas turbine engine compressor inner vane endwall application.

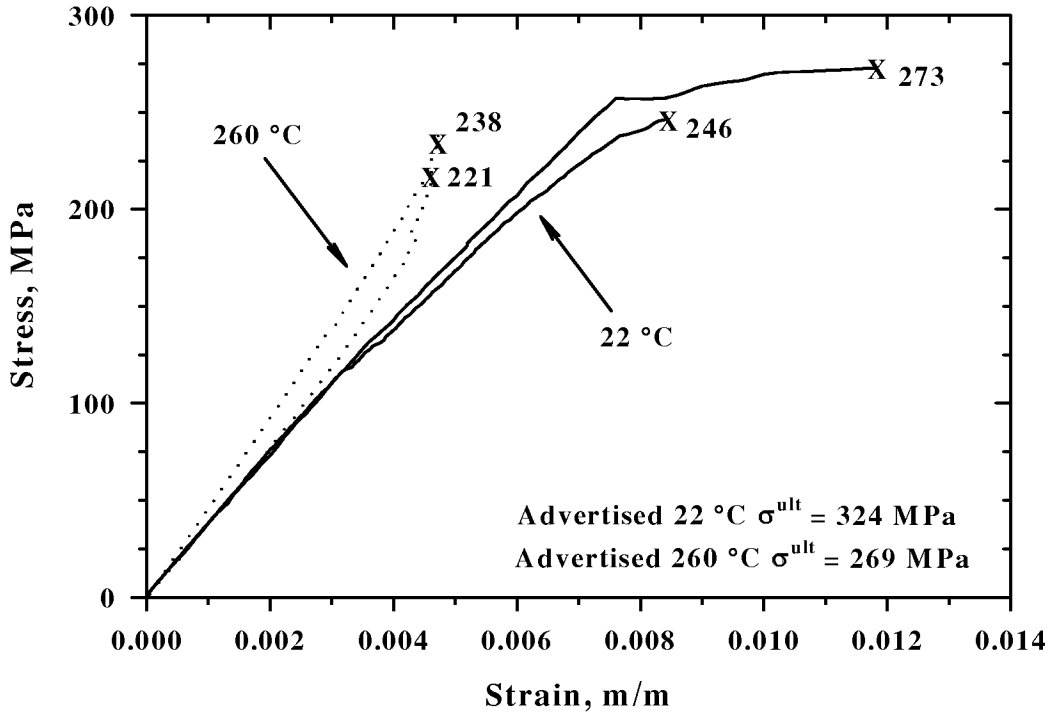

Figure 5—Static tensile behavior of as-manufactured T650-35/PMR-15 SMC at 22 and 260 °C.

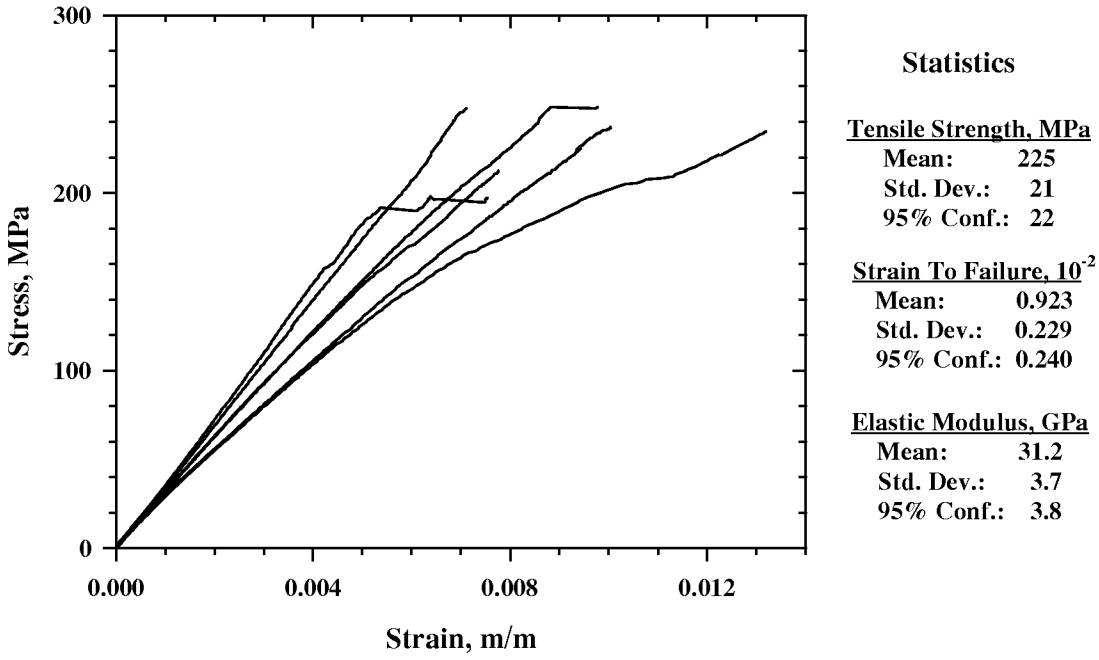

Figure 6—Static tensile behavior and property statistics of as-manufactured T650-35/PMR-15 SMC at 232 °C.

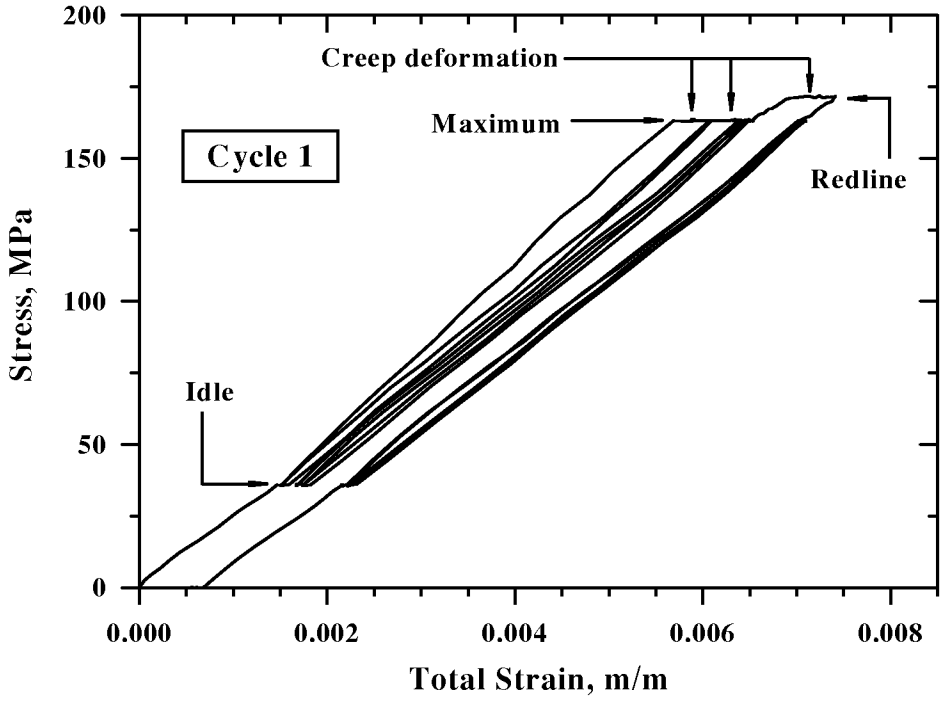

Figure 7—Stress/strain deformation behavior of T650-35/PMR-15 SMC with TMF mission cycle parameters established by $\sigma^{Max} = \sigma^{ult} - 3\Sigma$.

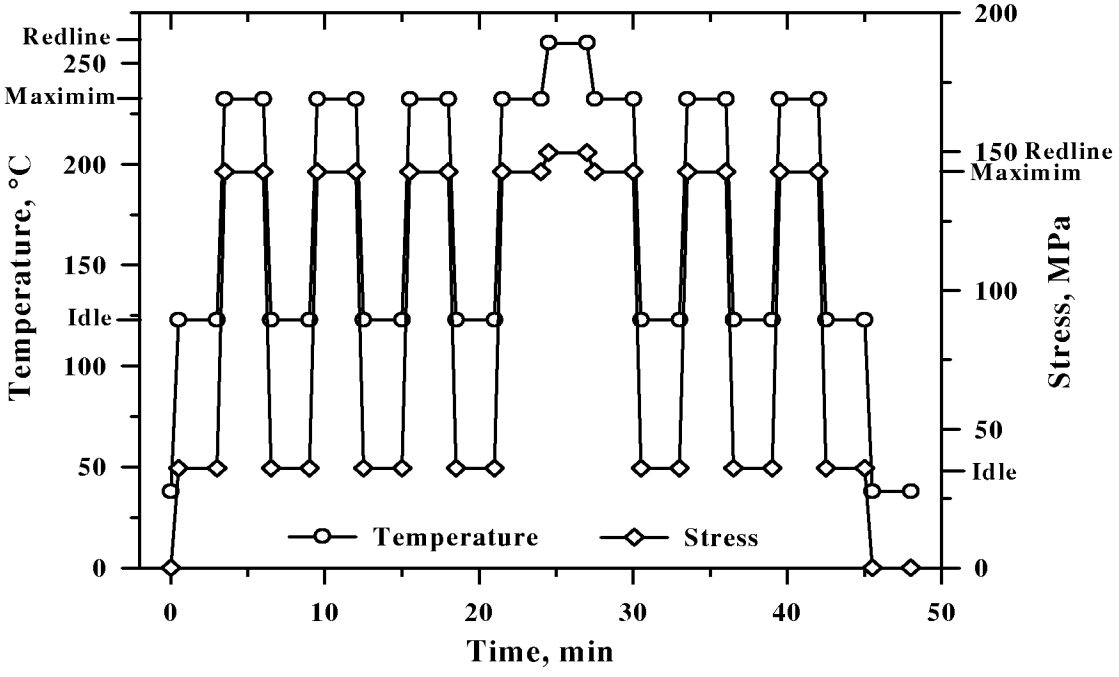

Figure 8—Finalized TMF mission cycle; parameters are based upon $\sigma^{Max} = \sigma^{ult} - 4\Sigma$.

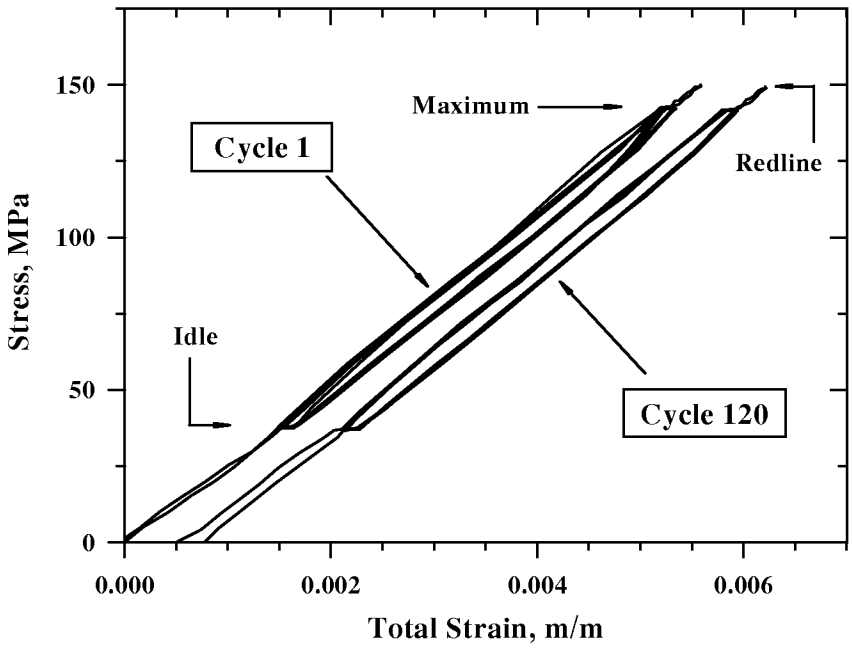

Figure 9—Stress/strain deformation behavior of T650-35/PMR-15 SMC with TMF mission cycle parameters established by $\sigma^{Max} = \sigma^{ult} - 4\Sigma$.

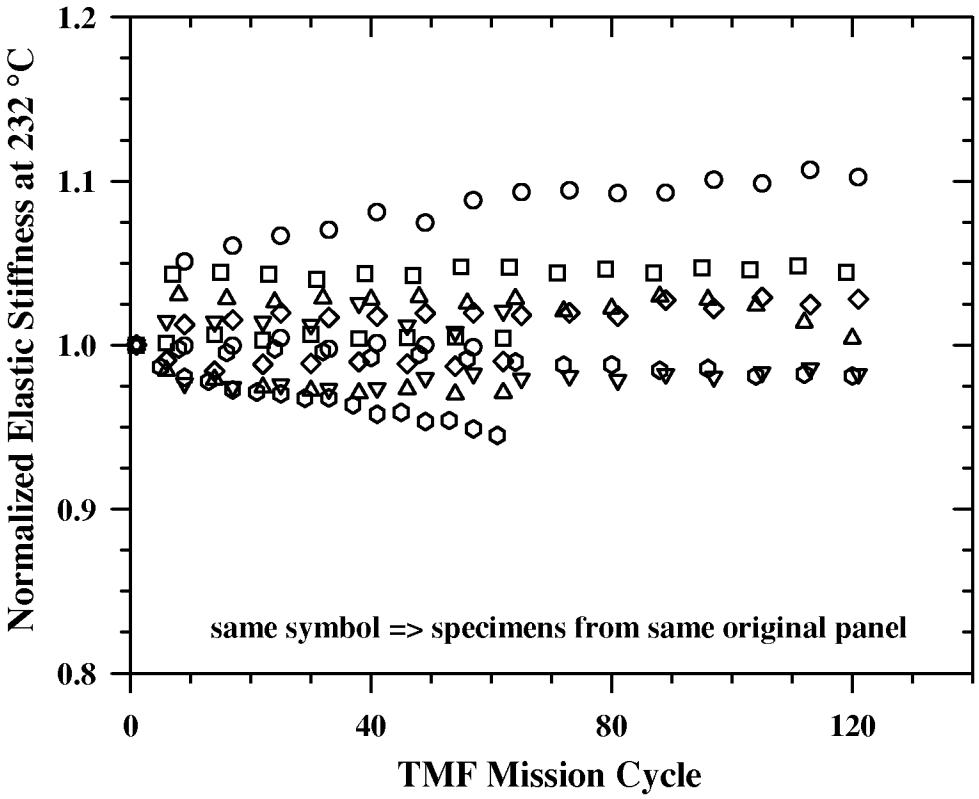

Figure 10—Normalized elastic stiffness measurements taken isothermally at 232 °C during TMF mission cycling.

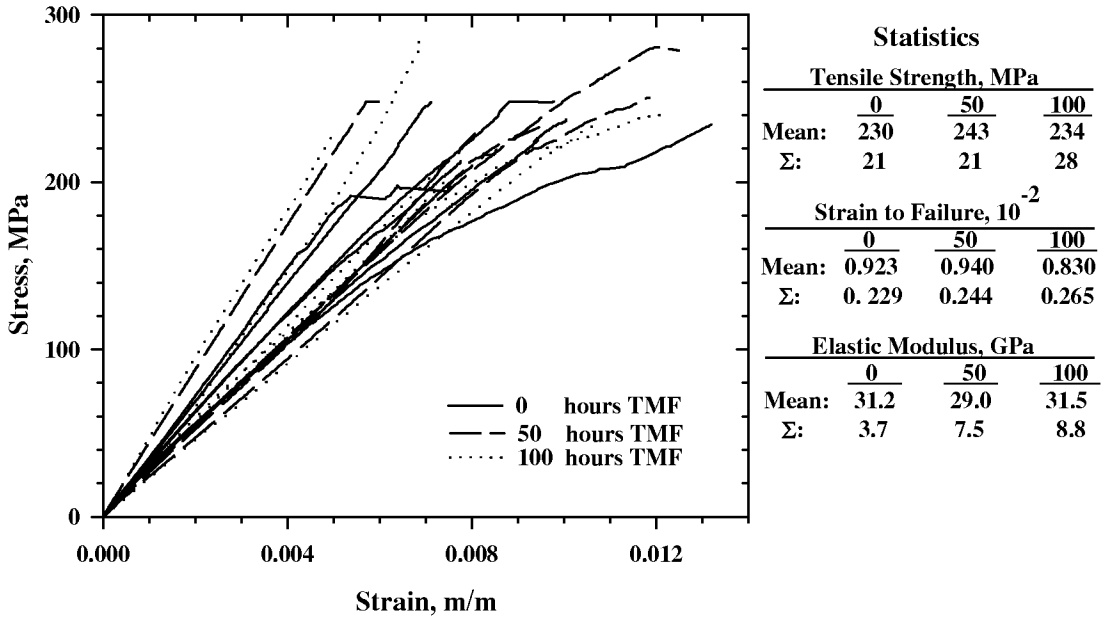

Figure 11—Residual static tensile properties at 232 °C subsequent to 50 and 100 hours of TMF mission cycling.

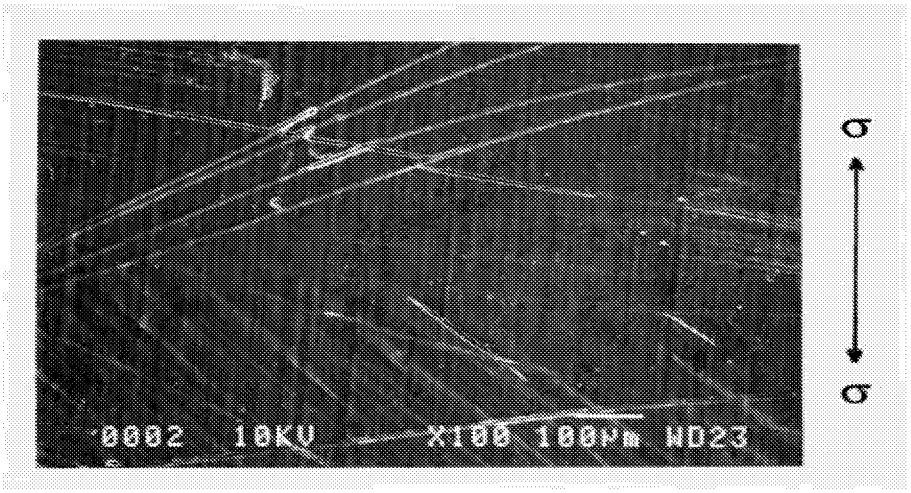

(a)

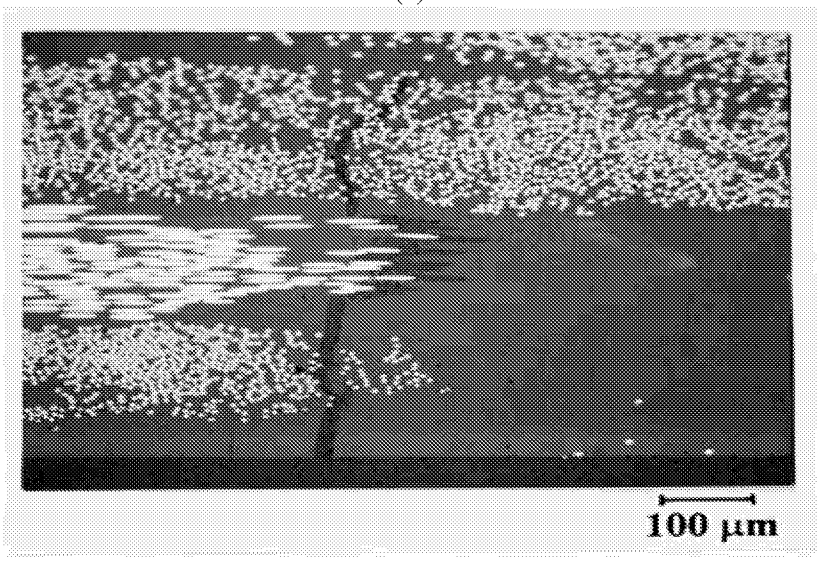

σ <————> σ (b)

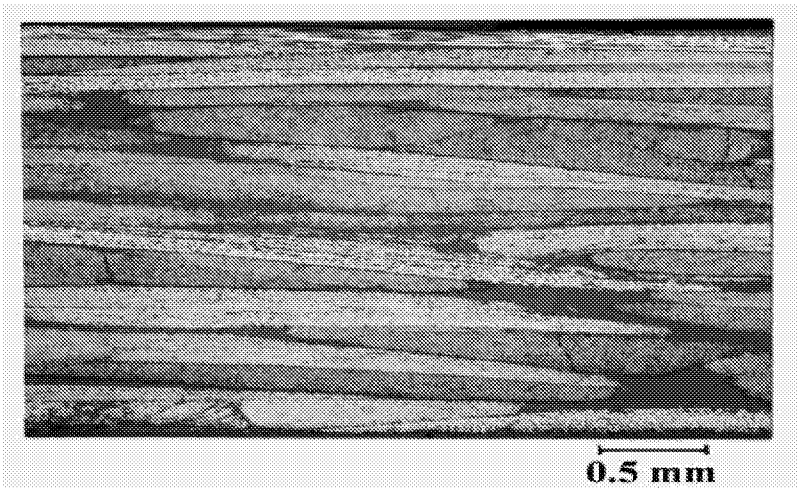

σ <————> σ (c)

Figure 12—SEM (a) and optical (b) & (c) microscopy revealing TMF damage in the SMC. (a) surface cracking associated with de-bonds; (b) view into specimen thickness revealing a transverse crack proceeding around the end of a predominantly longitudinal bundle; (c) view into specimen thickness showing transverse cracking associated with transversely oriented bundles.

Figure 13—Typical fracture surface of T650-35/PMR-15 SMC revealing extensive fiber and fiber bundle pull-out.

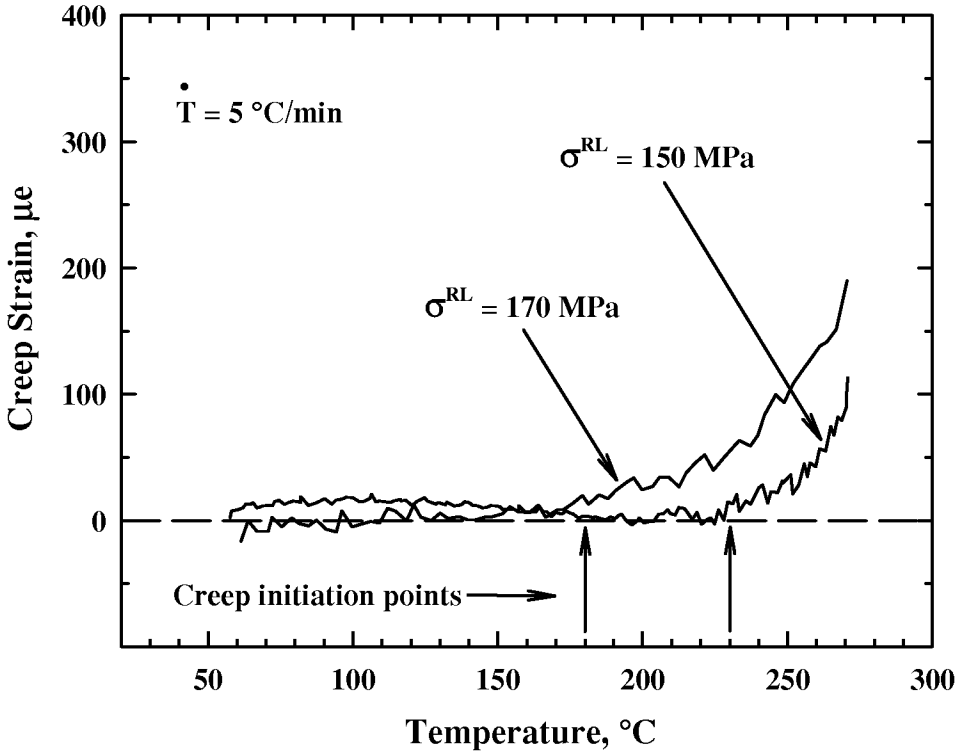

Figure 14—Thermomechanical creep threshold of T650-35/PMR-15 SMC at stress levels of 170 MPa (σ^{ult} - 3Σ) and 150 MPa (σ^{ult} - 4Σ).

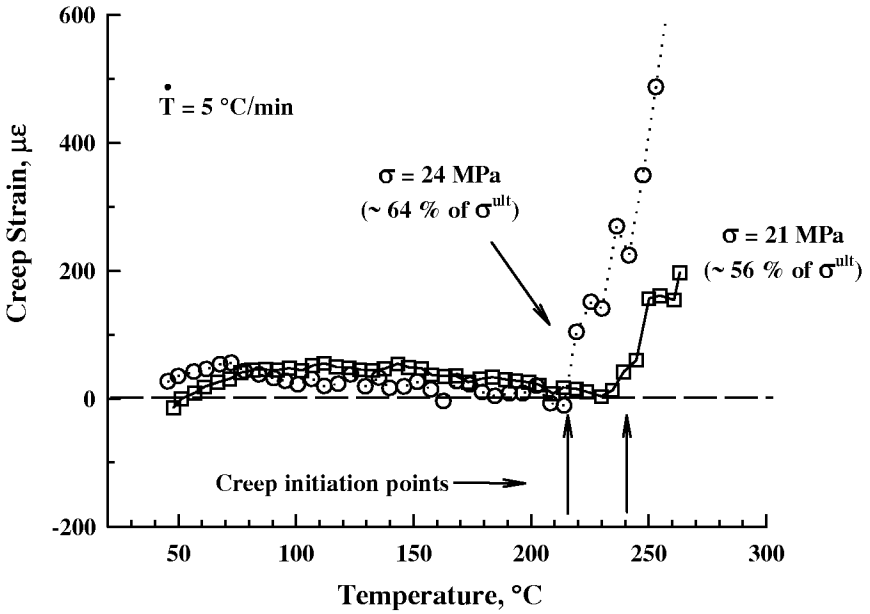

Figure 15—Thermomechanical creep threshold of neat PMR-15 at stress levels of 21 and 24 MPa, ~56 and 64 % of the 260°C σ^{ult}, respectively.

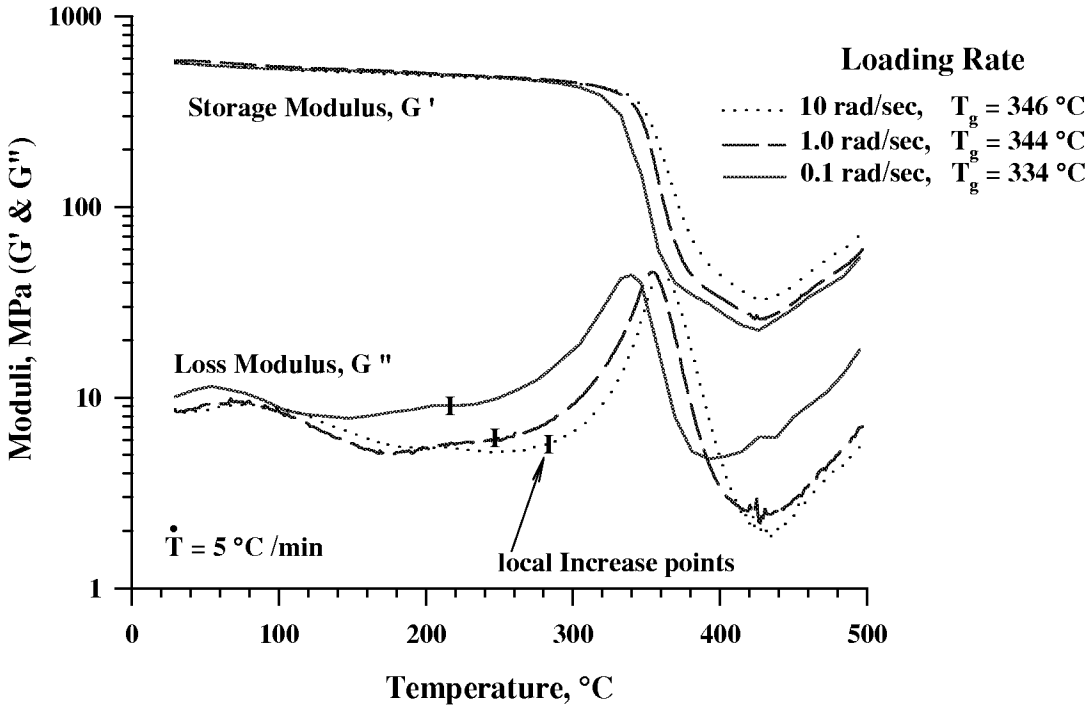

Figure 16—Loading rate dependent dynamic mechanical response of T650-35/PMR-15 SMC indicating dramatic shifts in T_g and G'' trends suggesting rate dependency at temperatures near 180 °C.

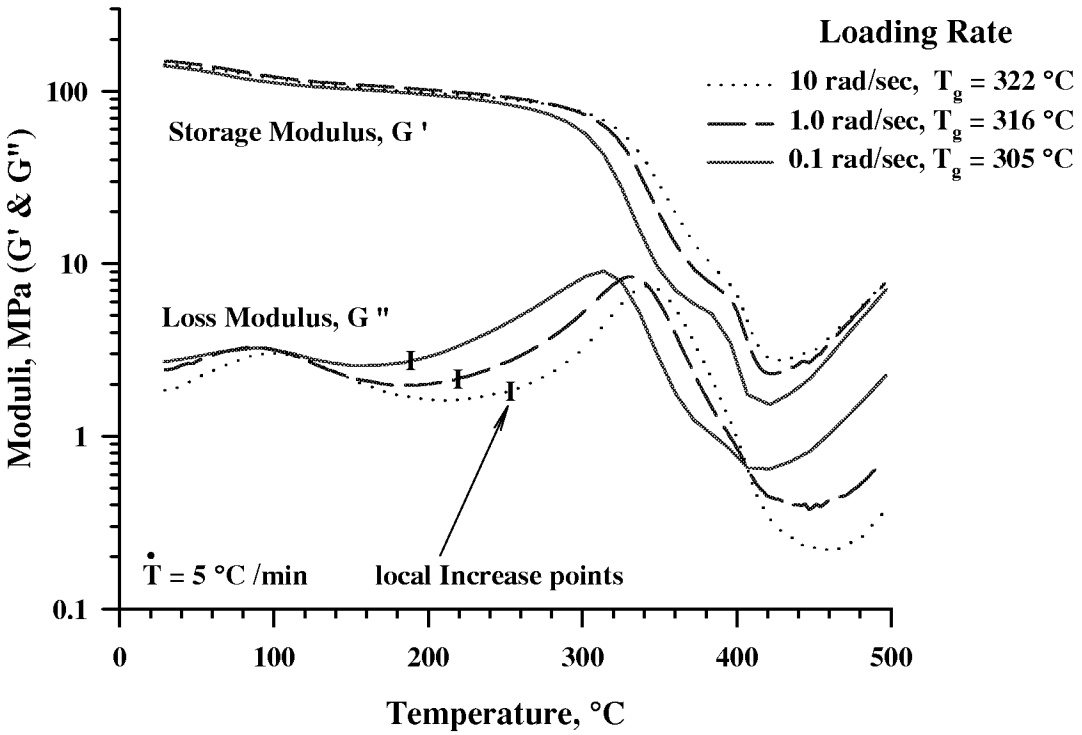

Figure 17—Loading rate dependent dynamic mechanical response of neat PMR-15 corroborating dramatic shifts in T_g and relatively low temperatures for rate dependency.

REPORT DOCUMENTATION PAGE

Form Approved
OMB No. 0704-0188

1. AGENCY USE ONLY (*Leave blank*)	2. REPORT DATE	3. REPORT TYPE AND DATES COVERED
	November 1998	Technical Memorandum

4. TITLE AND SUBTITLE

Thermomechanical Fatigue Durability of T650-35/PMR-15 Sheet Molding Compound

5. FUNDING NUMBERS

WU–523–21–13–00

6. AUTHOR(S)

Michael G. Castelli, James K. Sutter, and Dianne Benson

7. PERFORMING ORGANIZATION NAME(S) AND ADDRESS(ES)

National Aeronautics and Space Administration
Lewis Research Center
Cleveland, Ohio 44135–3191

8. PERFORMING ORGANIZATION REPORT NUMBER

E–11390

9. SPONSORING/MONITORING AGENCY NAME(S) AND ADDRESS(ES)

National Aeronautics and Space Administration
Washington, DC 20546–0001

10. SPONSORING/MONITORING AGENCY REPORT NUMBER

NASA TM—1998-208806

11. SUPPLEMENTARY NOTES

Prepared for the Symposium on Time-Dependent and Non-Linear Effects in Polymers and Composites sponsored by the American Society for Testing and Materials, Atlanta, Georgia, May 4–5, 1998. Michael G. Castelli, Ohio Aerospace Institute, 22800 Cedar Point Road, Cleveland, Ohio 44142; James K. Sutter, NASA Lewis Research Center; Dianne Benson, ProTech Lab Corporation, Cincinnati, Ohio. Responsible person, Michael G. Castelli, organization code 5920, (216) 433–8464.

12a. DISTRIBUTION/AVAILABILITY STATEMENT

Unclassified - Unlimited
Subject Category: 24 Distribution: Nonstandard

This publication is available from the NASA Center for AeroSpace Information, (301) 621–0390.

12b. DISTRIBUTION CODE

13. ABSTRACT ***(Maximum 200 words)***

Although polyimide based composites have been used for many years in a wide variety of elevated temperature applications, very little work has been done to examine the durability and damage behavior under more prototypical thermomechanical fatigue (TMF) loadings. Synergistic effects resulting from simultaneous temperature and load cycling can potentially lead to enhanced, if not unique, damage modes and contribute to a number of nonlinear deformation responses. The goal of this research was to examine the effects of a TMF loading spectrum, representative of a gas turbine engine compressor application, on a polyimide sheet molding compound (SMC). High performance SMCs present alternatives to prepreg forms with great potential for low cost component production through less labor intensive, more easily automated manufacturing. To examine the issues involved with TMF, a detailed experimental investigation was conducted to characterize the durability of a T650–35/PMR–15 SMC subjected to TMF mission cycle loadings. Fatigue damage progression was tracked through macroscopic deformation and elastic stiffness. Additional properties, such as the glass transition temperature (T_g) and dynamic mechanical properties were examined. The fiber distribution orientation was also characterized through a detailed quantitative image analysis. Damage tolerance was quantified on the basis of residual static tensile properties after a prescribed number of TMF missions. Detailed microstructural examinations were conducted using optical and scanning electron microscopy to characterize the local damage. The imposed baseline TMF missions had only a modest impact on inducing fatigue damage with no statistically significant degradation occurring in the measured macroscopic properties. Microstructural damage was, however, observed subsequent to 100 h of TMF cycling which consisted primarily of fiber debonding and transverse cracking local to predominantly transverse fiber bundles. The TMF loadings did introduce creep related effects (strain accumulation) which led to rupture in some of the more aggressive stress scenarios examined. In some cases this creep behavior occurred at temperatures in excess of 150 °C below commonly cited values for T_g. Thermomechanical exploratory creep tests revealed that the SMC was subject to time dependent deformation at stress/temperature thresholds of 150 MPa/230 °C and 170 MPa/180 °C.

14. SUBJECT TERMS

Polymer matrix composite; Fatigue; Damage; Residual strength; Tensile properties

15. NUMBER OF PAGES

29

16. PRICE CODE

A03

17. SECURITY CLASSIFICATION OF REPORT	18. SECURITY CLASSIFICATION OF THIS PAGE	19. SECURITY CLASSIFICATION OF ABSTRACT	20. LIMITATION OF ABSTRACT
Unclassified	Unclassified	Unclassified	